

Electronic Supporting Information:

Cu nanocrystals enhancement of C₃N₄/Cu hetero-structure and new application on photo-electronic catalysis: hydrazine oxidation and redox reaction of organic molecule

Muwei Ji,^{a,b} Jintao Huang,^{a,b} Yiqing He,^c Dongsheng He,^d Donghai Luo,^a Erhuang Zhang,^e Meng Xu,^e Jia Liu,^e Jiatao Zhang,^e Bo Li,^c Jian Xu,^b Jin Wang,^c and Caizhen Zhua,^{*}

- College of chemistry and environment engineering, Shenzhen University, Shenzhen, 518060, P. R. China.
- Institute of Chemistry, Chinese Academy of Sciences, Beijing, 100190, P.R. China.
- Graduate School at Shenzhen, Tsinghua University, Shenzhen, 518055, P.R. China.
- Southern University of science and technology, Shenzhen, 518055, P.R. China.
- Beijing institute of technology, Beijing, 100081, P.R. China.

Figure S1-S11 and Table S1-S2

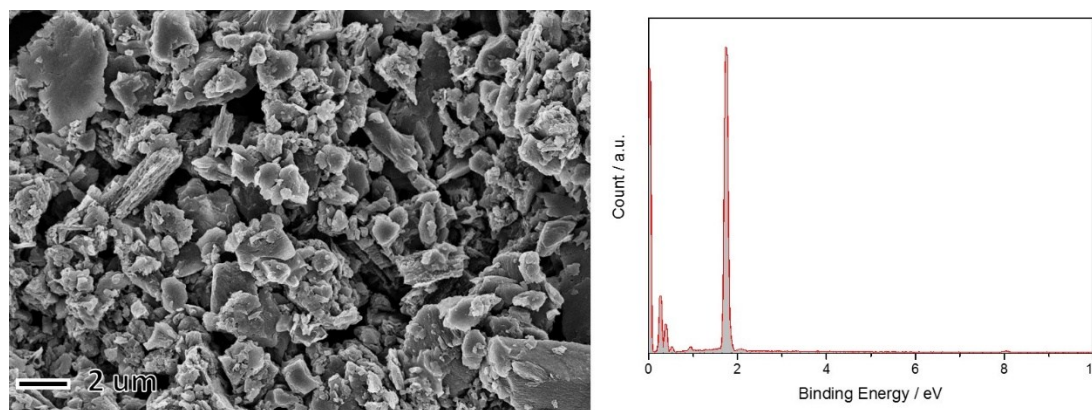


Figure S1. SEM images of as-prepared products after the reaction between C₃N₄/Cu hetero-structure; B) the according EDS analysis.

Table S1. Cu concentration of C₃N₄/Cu, characterized by ICP. The test solution was prepared by employing 99.3 mg of as-prepared C₃N₄/Cu to dissolve in HNO₃ then the resulted solution was diluted into 10 mL with water.

Element	Concentration of Cu (mg/L)	S.D.
Cu	5.99	0.01

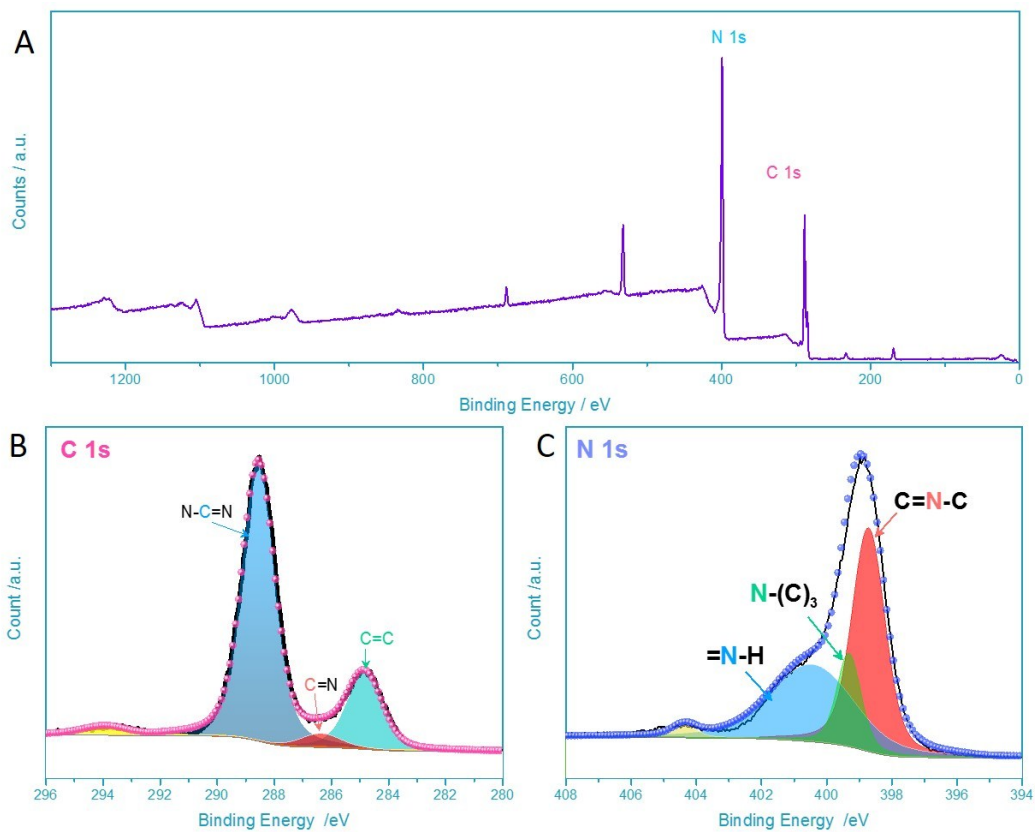


Figure S2. Survey XPS of as-prepared C_3N_4 powder and the corresponding high resolution XPS spectra of B) C 1s and C) N 1s.

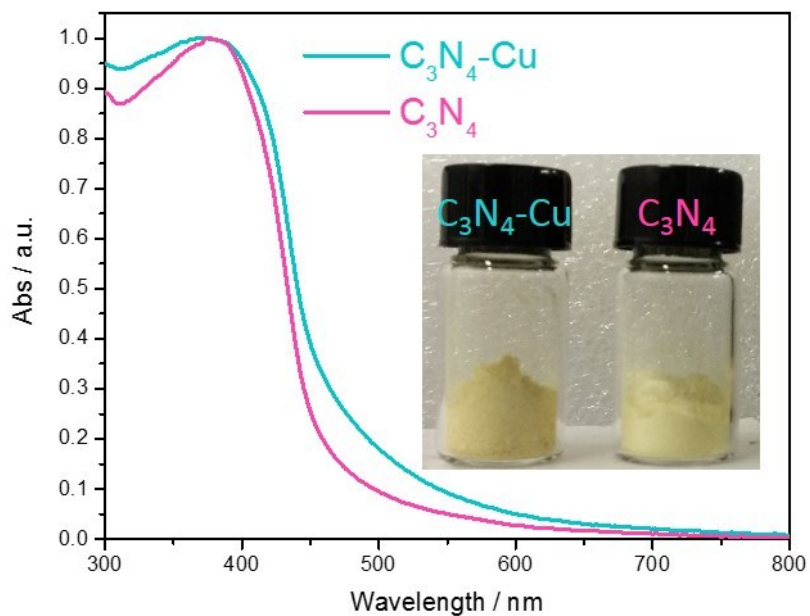


Figure S3. The UV-visual absorption spectra of C_3N_4/Cu hetero structure and graphitic C_3N_4 electrode.

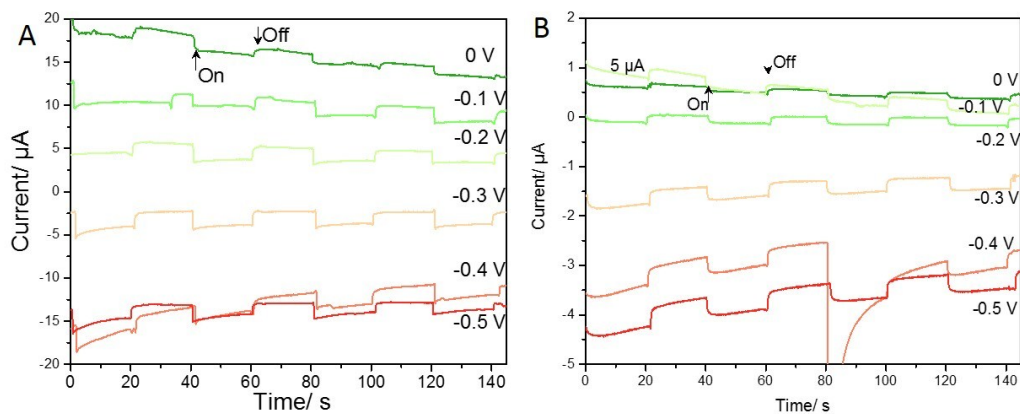


Figure S4. The photocurrent of $\text{C}_3\text{N}_4/\text{Cu}$ hetero structure (A) and graphitic C_3N_4 electrode (B).

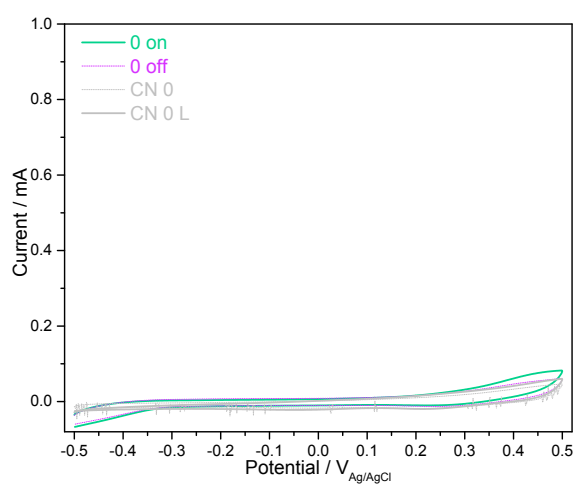


Figure S5. The CV plots of $\text{C}_3\text{N}_4/\text{Cu}$ hetero structure and graphitic C_3N_4 electrode with hydrazine free.

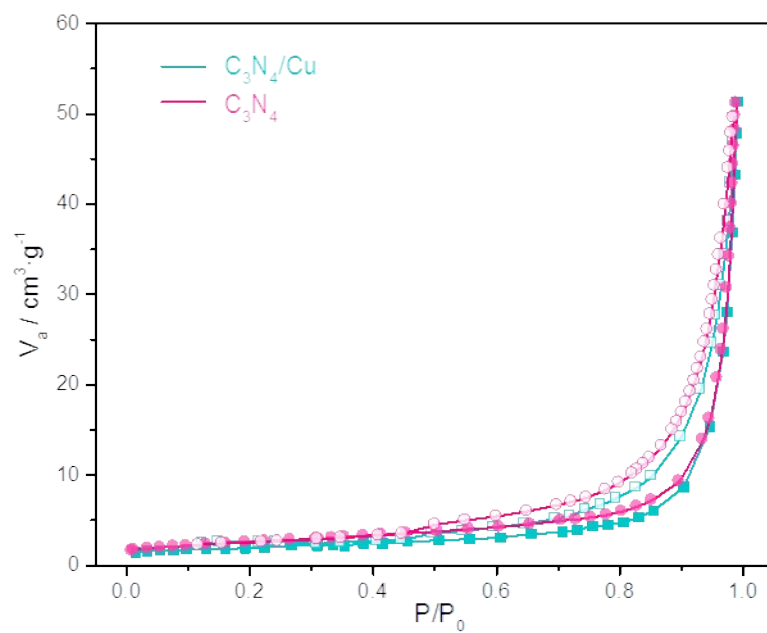


Figure S6. N_2 sorption isotherms of $\text{C}_3\text{N}_4/\text{Cu}$ and graphitic C_3N_4 .

Table S2. BET characterization of as-prepared of C_3N_4/Cu and graphitic C_3N_4 , which showed the surface of graphitic C_3N_4 was closed to that of C_3N_4/Cu hetero-structure.

C_3N_4/Cu	
V_m	1.6163 [cm ³ (STP) g ⁻¹]
$a_{s,BET}$	7.035 [m ² g ⁻¹]
C	304.16
Total pore volume($p/p_0=0.990$)	0.07683 [cm ³ g ⁻¹]
Mean pore diameter	43.685 nm
C_3N_4	
V_m	2.156 [cm ³ (STP) g ⁻¹]
$a_{s,BET}$	9.384 [m ² g ⁻¹]
C	88.625
Total pore volume($p/p_0=0.990$)	0.078712 [cm ³ g ⁻¹]
Mean pore diameter	33.551 nm

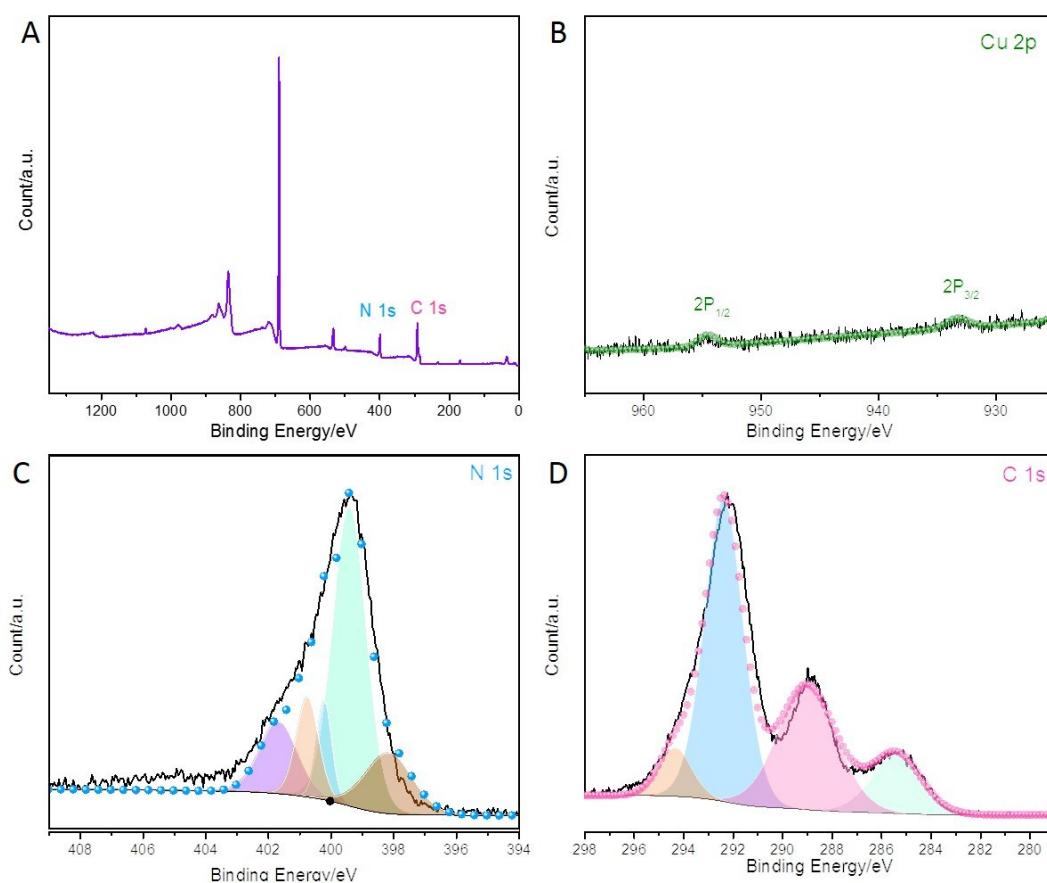


Figure S7. The XPS spectrum of as-prepared C_3N_4/Cu hetero-structure after photo-electronic reaction: (A) survey spectra and high resolution XPS, (B) Cu 2p, (C) N 1s, and (D) C 1s.

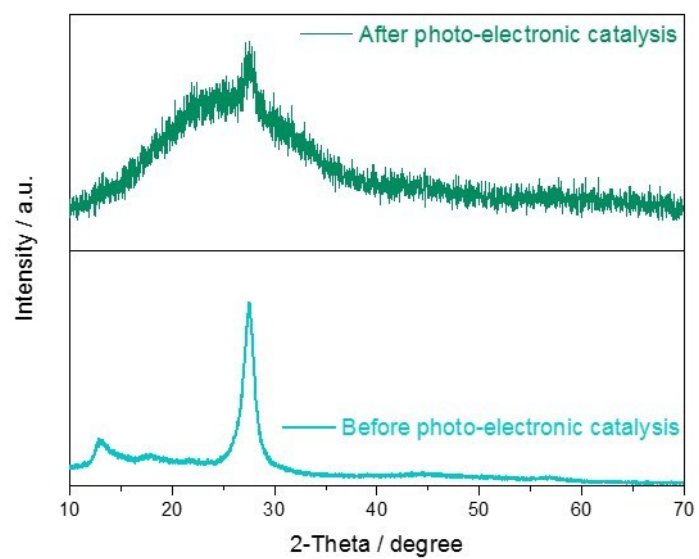


Figure S8. XRD pattern comparing of C_3N_4/Cu hetero-structure before and after photo-electronic catalysis.

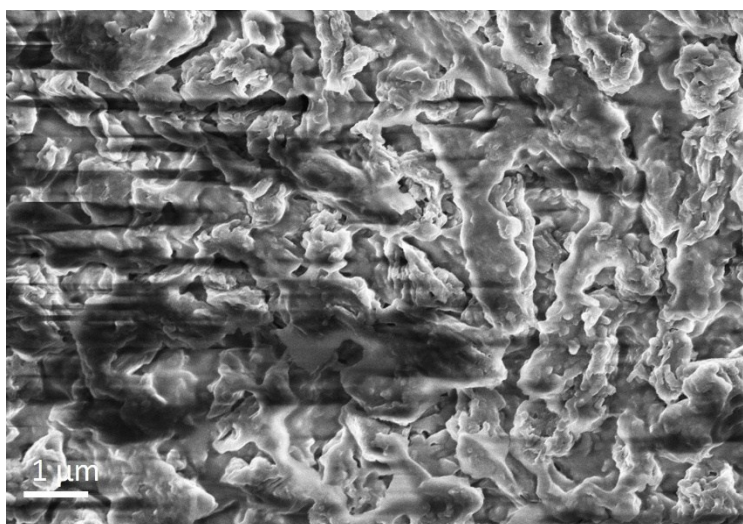


Figure S9. The TEM images of as-prepared C_3N_4/Cu hetero-structure after photo-electronic catalysis.

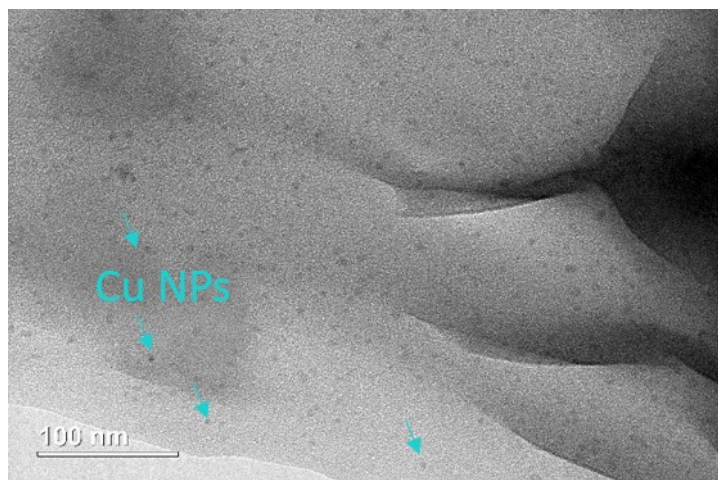


Figure S10. The TEM images of as-prepared C_3N_4/Cu hetero-structure after photo-electronic catalysis.

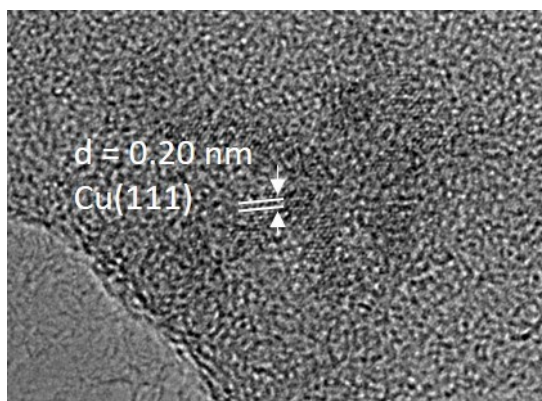


Figure S11. The HRTEM images of as-prepared C_3N_4/Cu hetero-structure before and after photo-electronic catalysis.